Haogen Huang

Mechanical and Aerospace Portfolio

Columbia University, M.S. Mechanical Engineering
CAD, prototyping, CFD, FEA, wind tunnel and test validation
New York, NY | hh3172@columbia.edu | linkedin.com/in/haogenhuang

Engineering Range & Skills

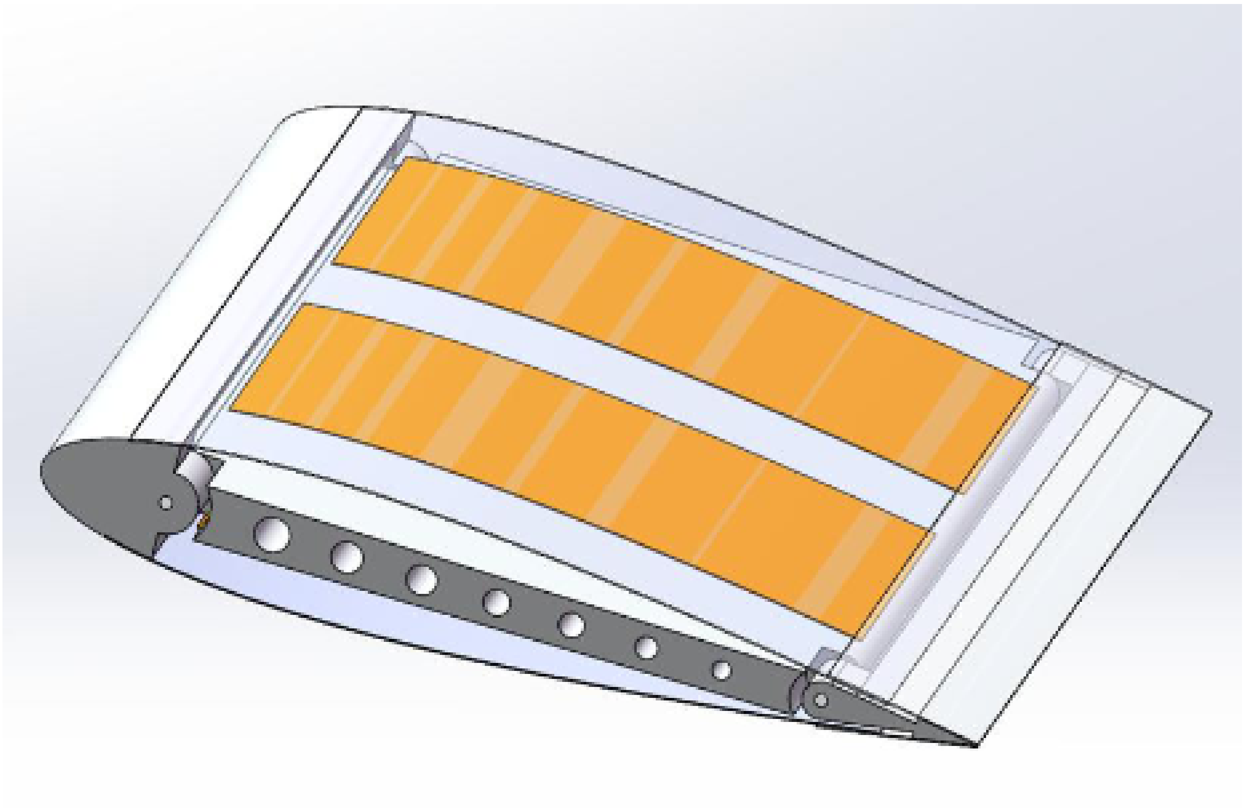

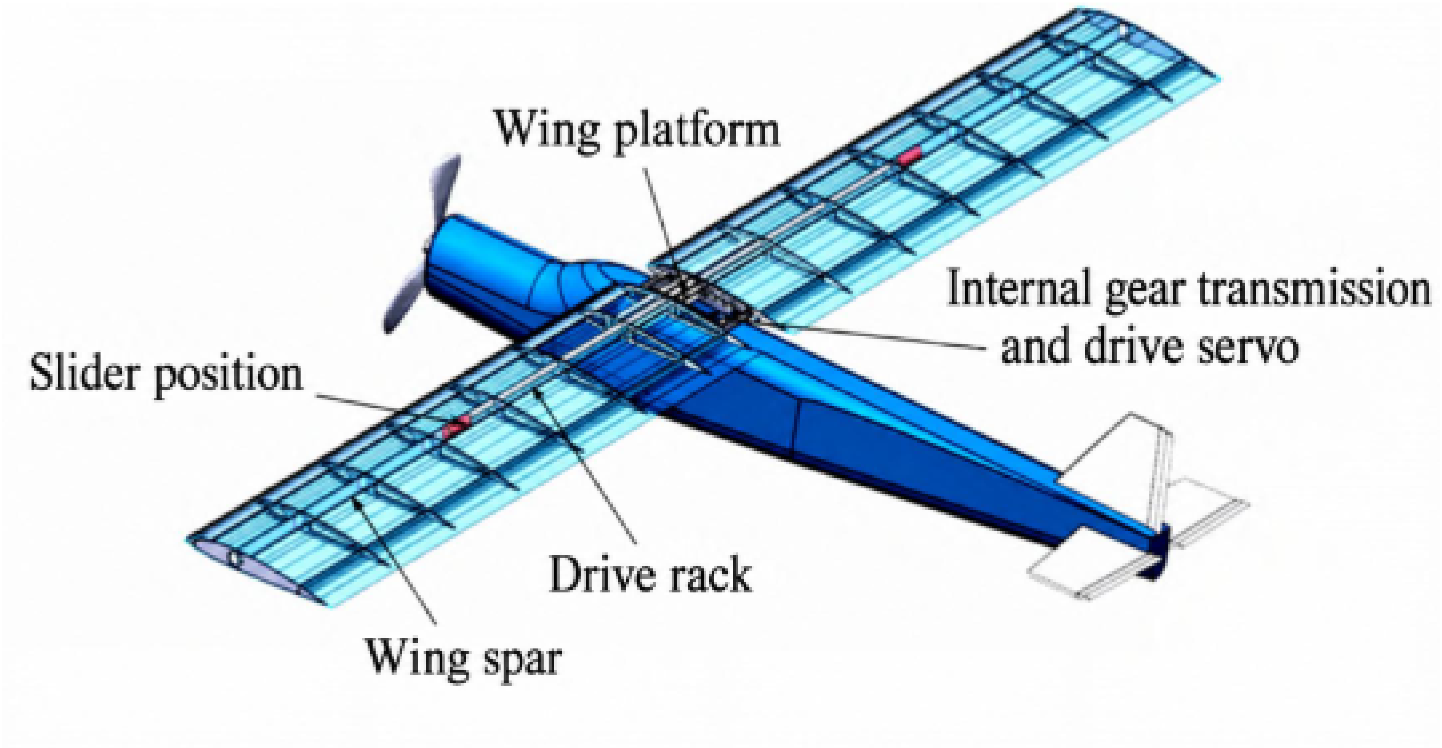

Smart-material morphing wing

Tandem-wing lifting-body payload aircraft

Fluid-driven moving-mass control aircraft

- **CAD + CFD + FEA**
  SolidWorks/AutoCAD, CATIA, Fluent, ANSYS, Simcenter STAR-CCM+
- **Build + Test**
  3D Printing, CNC Machining, Laser Cutting, Wind tunnel, Flight tests
- **Control**
  Pixhawk/QGroundControl, MFC actuation, moving CG
- **Analyze**
  Python, Matlab

Smart-material morphing wing

Lightweight adaptive airfoil prototype with flexible carbon-fiber skin and bonded MFC actuators.

- The morphing wing geometry is based on the NACA 0015 airfoil, with a chord length of 150 mm and a wingspan of 200 mm.
- The wing skin is made of 0.3 mm carbon fiber material, with two M8557-P1 type MFC smart material patches bonded to each side of the wing skin.
- The skin can slide within the adjustment channel at the trailing edge.

Trailing-edge sliding morphing wing

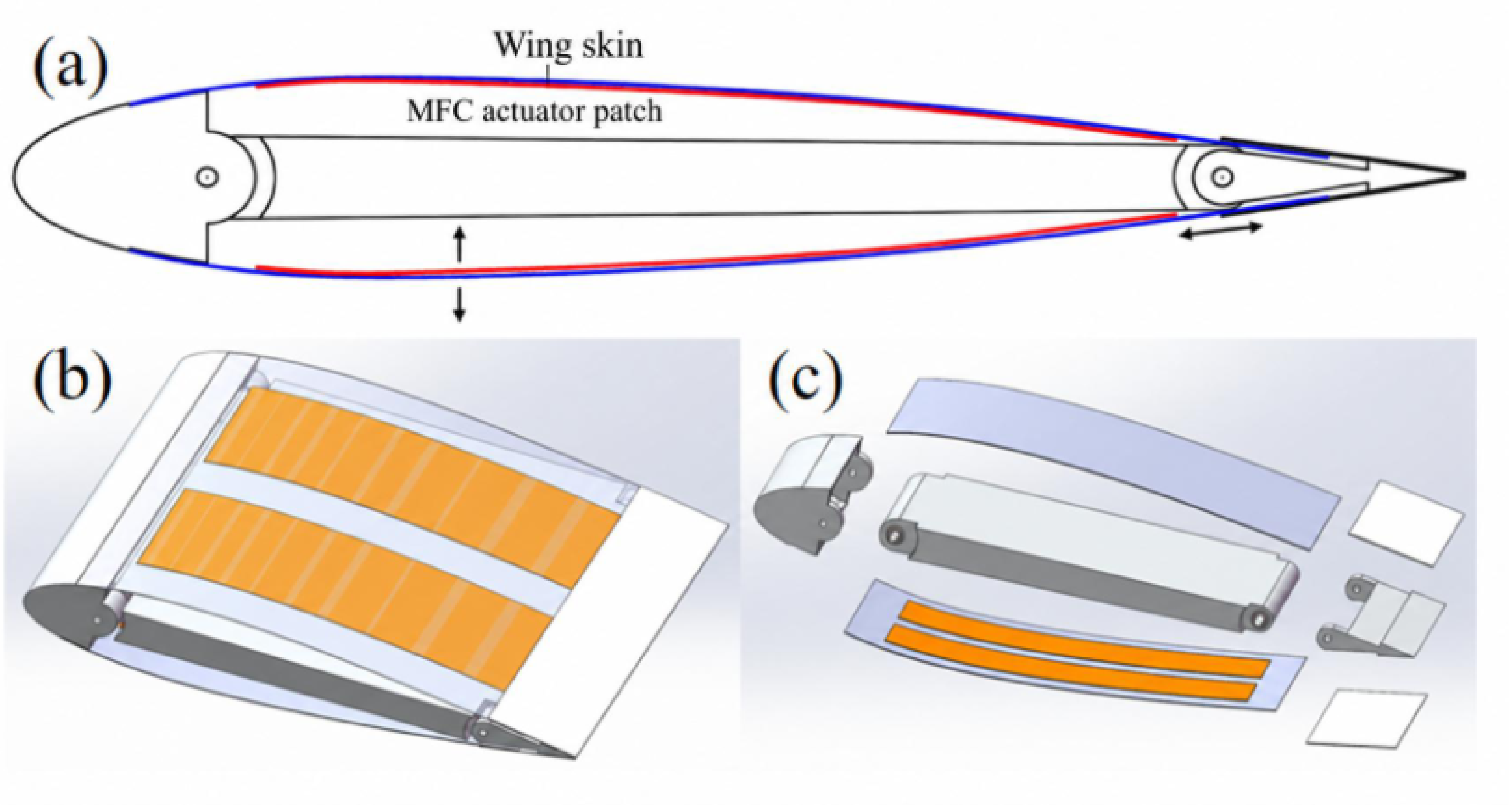

(a) Schematic diagram of the morphing principle
(b) Assembly schematic
(c) Exploded view

Leading-edge sliding morphing wing

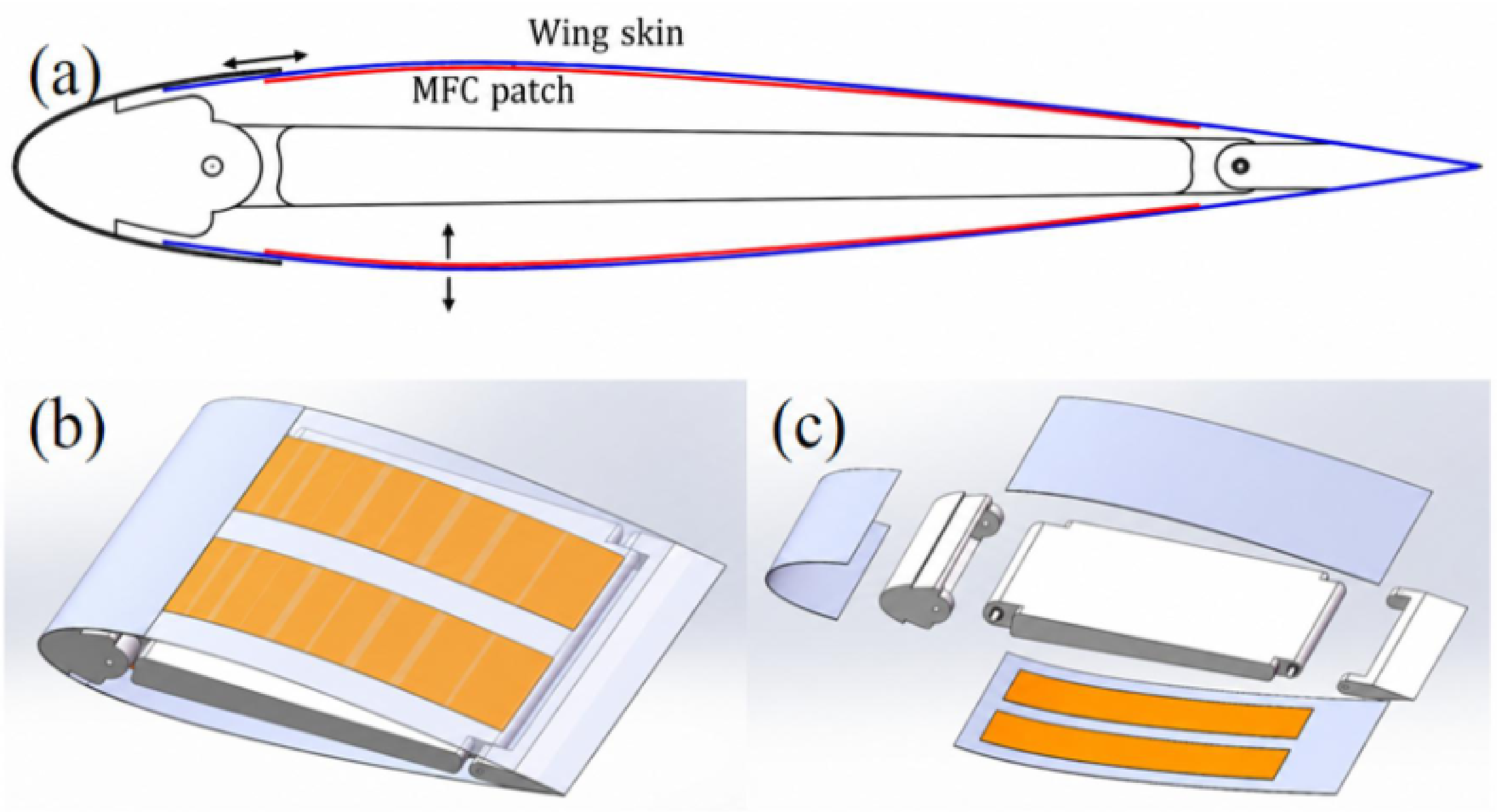

(a) Schematic diagram of the morphing principle
(b) Assembly schematic
(c) Exploded view

Smart-material morphing wing

Lightweight adaptive airfoil prototype with flexible carbon-fiber skin and bonded MFC actuators.

Morphing Wing Wind Tunnel Test Platform

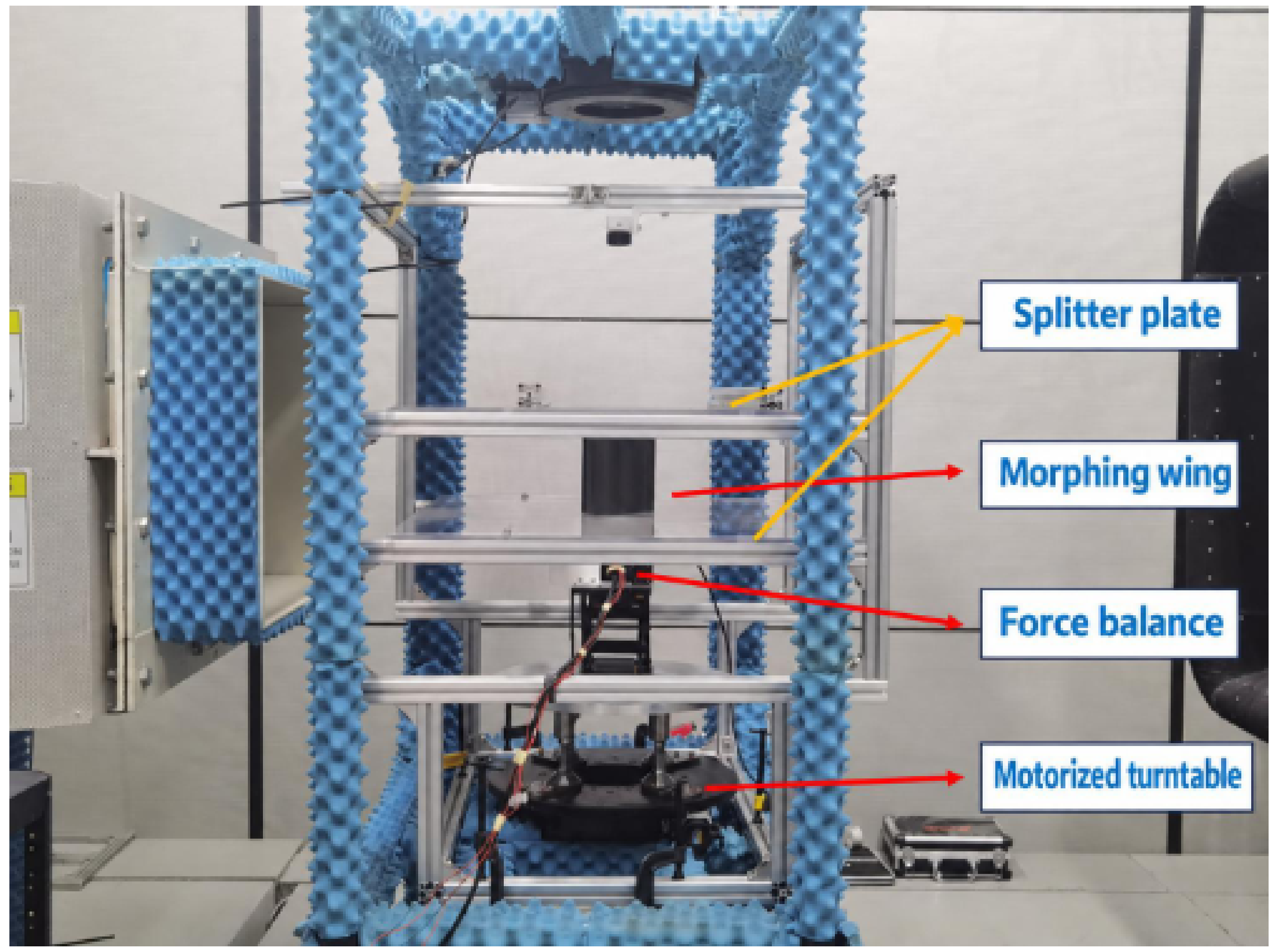

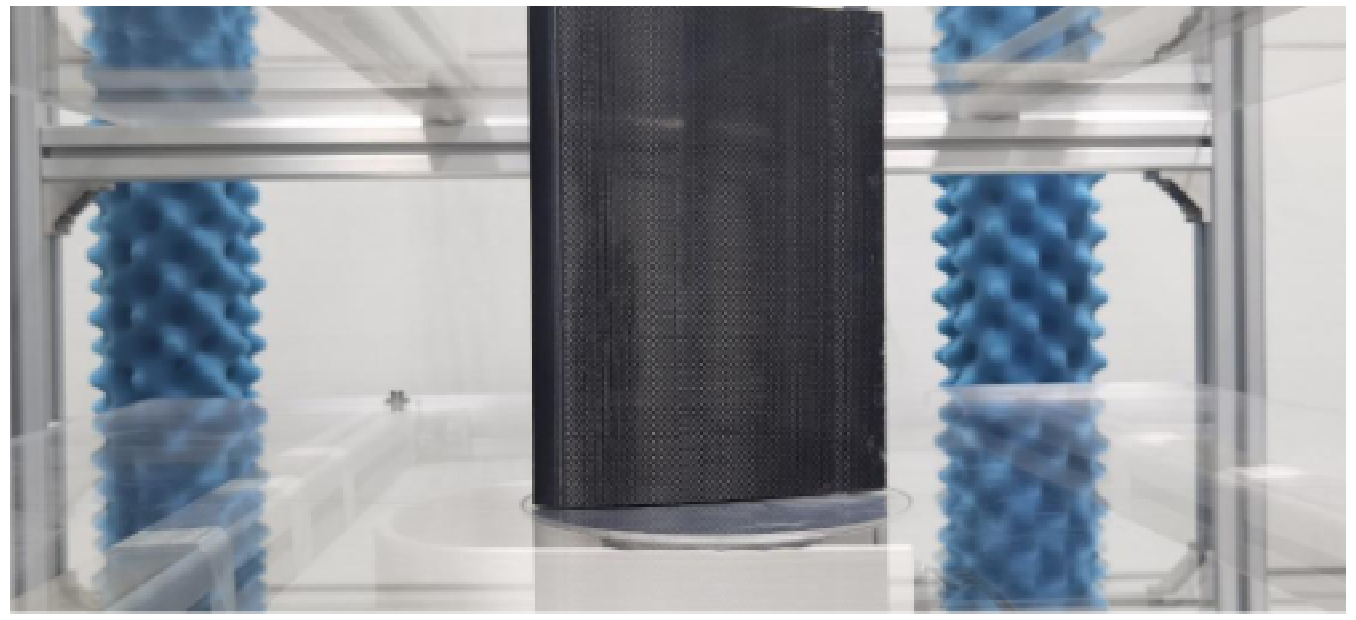

Line charts of partial experimental data for the trailing-edge sliding morphing wing

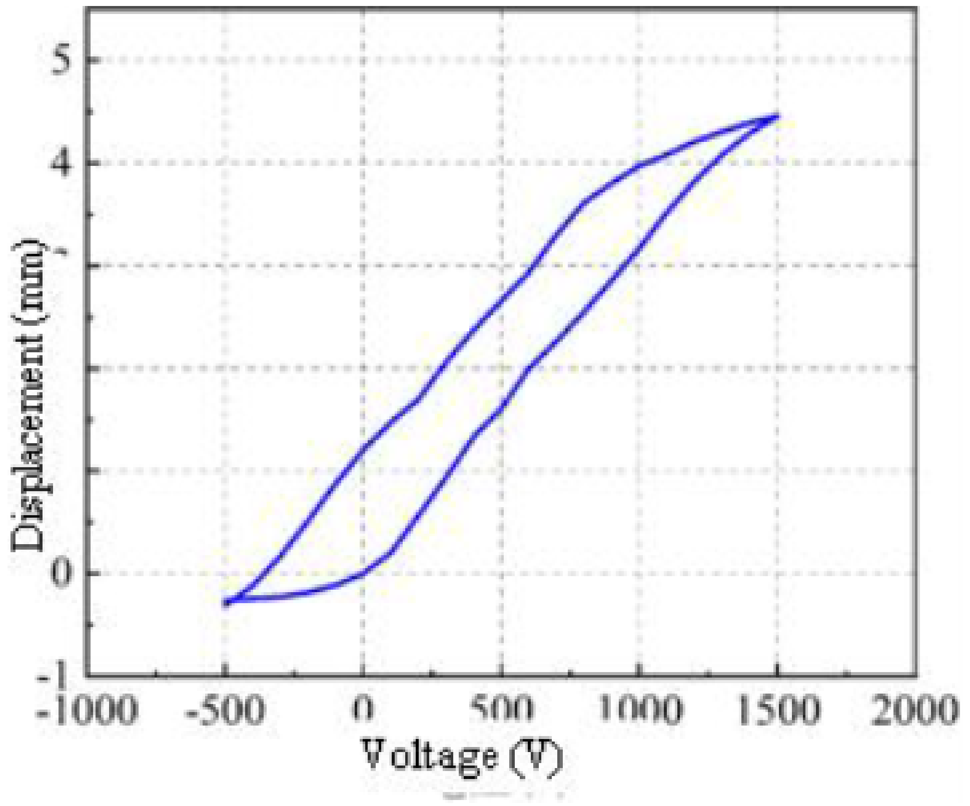

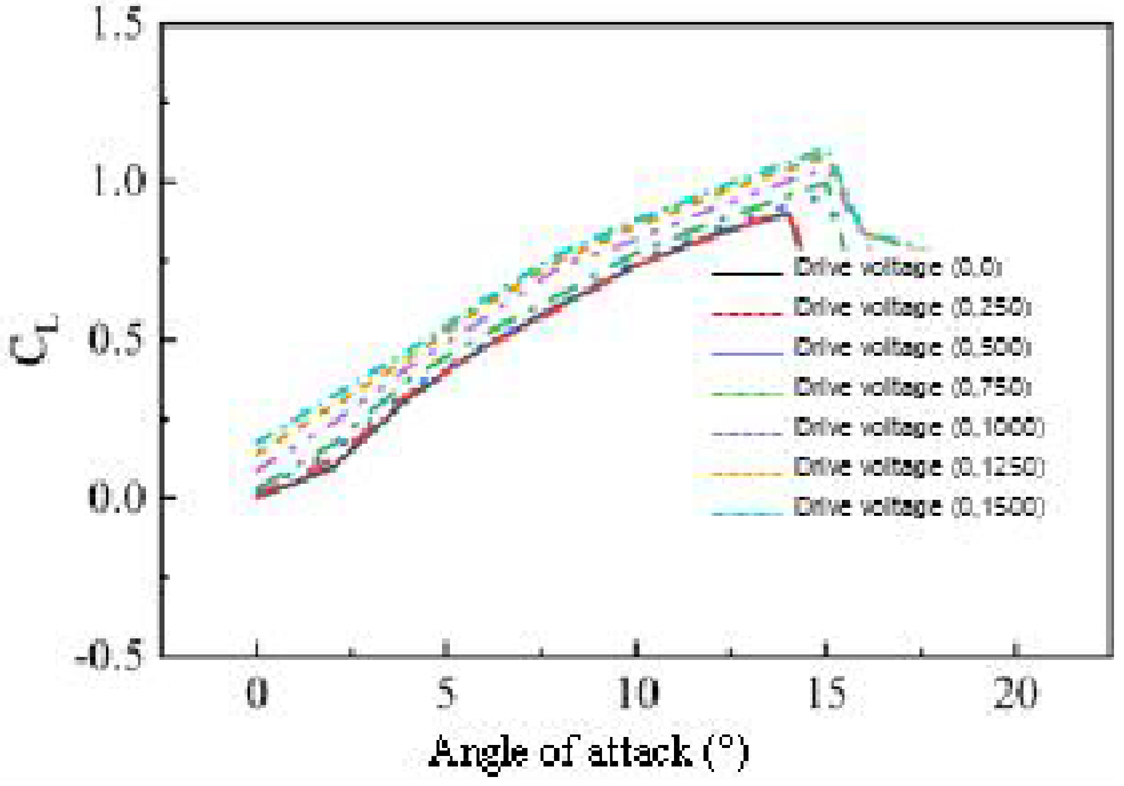

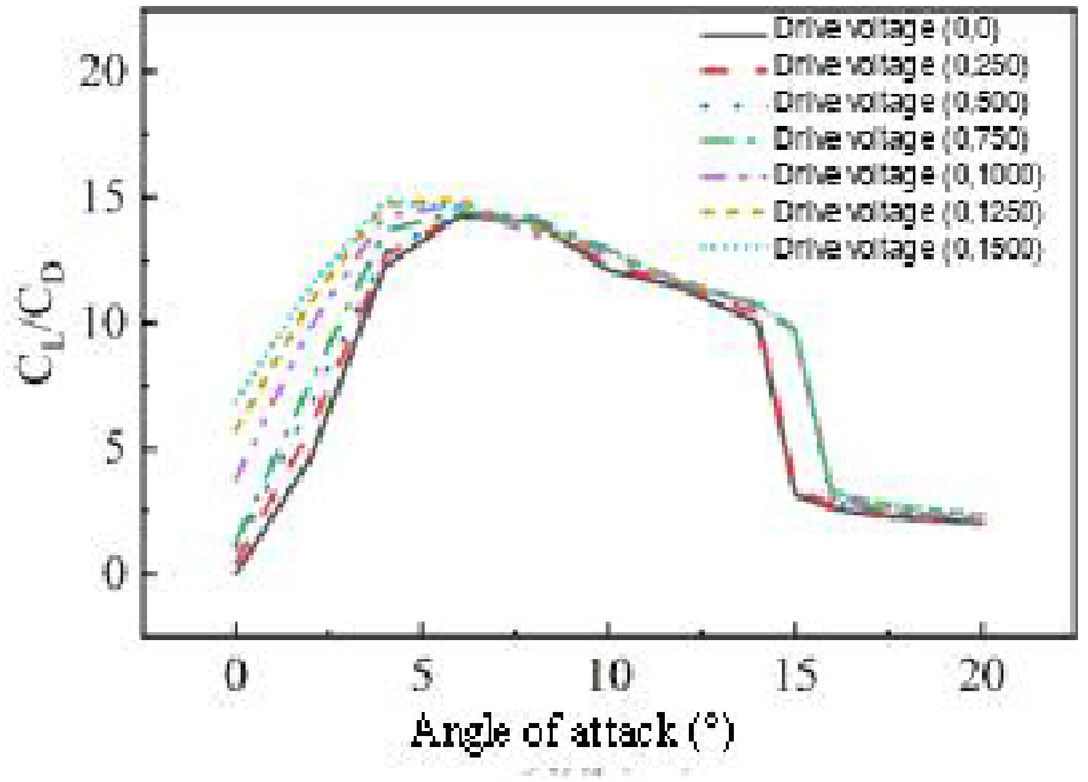

- 500 to 1500 V
MFC drive-voltage sweep

5 points at 0.4c
spanwise uniformity measurement

15 / 20 / 30 m/s
wind-tunnel flow speeds

➢ Validated outcome

- Demonstrated smooth and effective MFC-driven wing morphing under different actuation voltages.
- Increased the maximum lift coefficient by 27.8% for the trailing-edge sliding wing and 34.9% for the leading-edge sliding wing.
- Improved low-angle lift-to-drag ratio by about 150% and delayed stall angle by 2°.

Tandem-wing lifting-body payload aircraft

Project leader, China Universities Aircraft Design Competition, 2022 to 2023

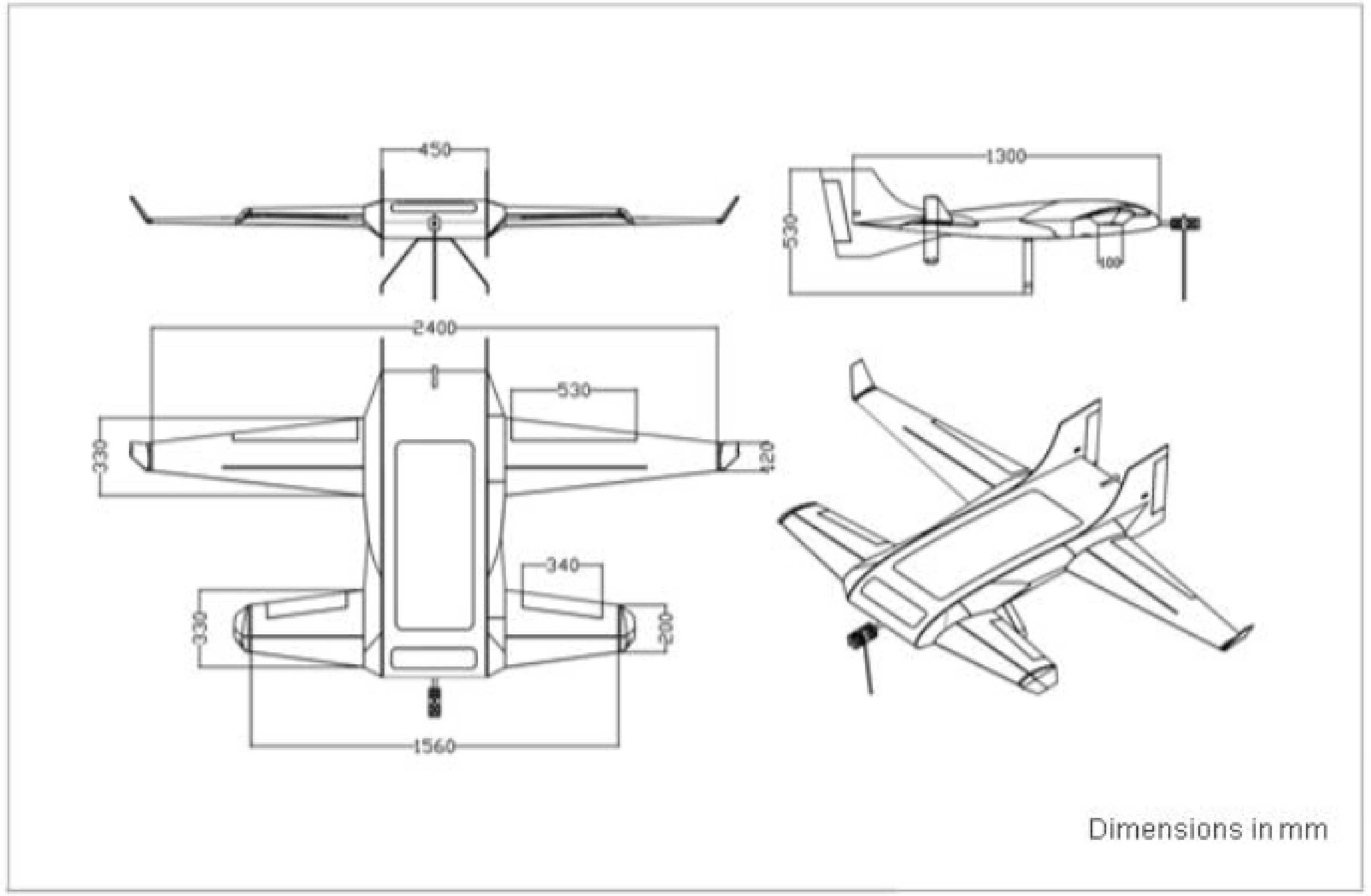

2.4 m	maximum wingspan
1.3 m	aircraft length
6-10 kg	target takeoff weight
110 tennis balls	payload target
14-18 m/s	target cruise speed

- A tandem-wing lifting-body layout packaged the payload inside the aerodynamic body instead of adding an under-wing cargo pod.
- The configuration combined distributed lifting surfaces and four-surface mixed control to maintain stability and maneuverability under heavy load.

Tandem-wing lifting-body payload aircraft

Mission constraints drove the tandem-wing lifting-body configuration

1. CONFIGURATION SELECTION

Design problem: carry a large payload of tennis balls within an appropriate wingspan, while maintaining low cruise drag and trim penalties.

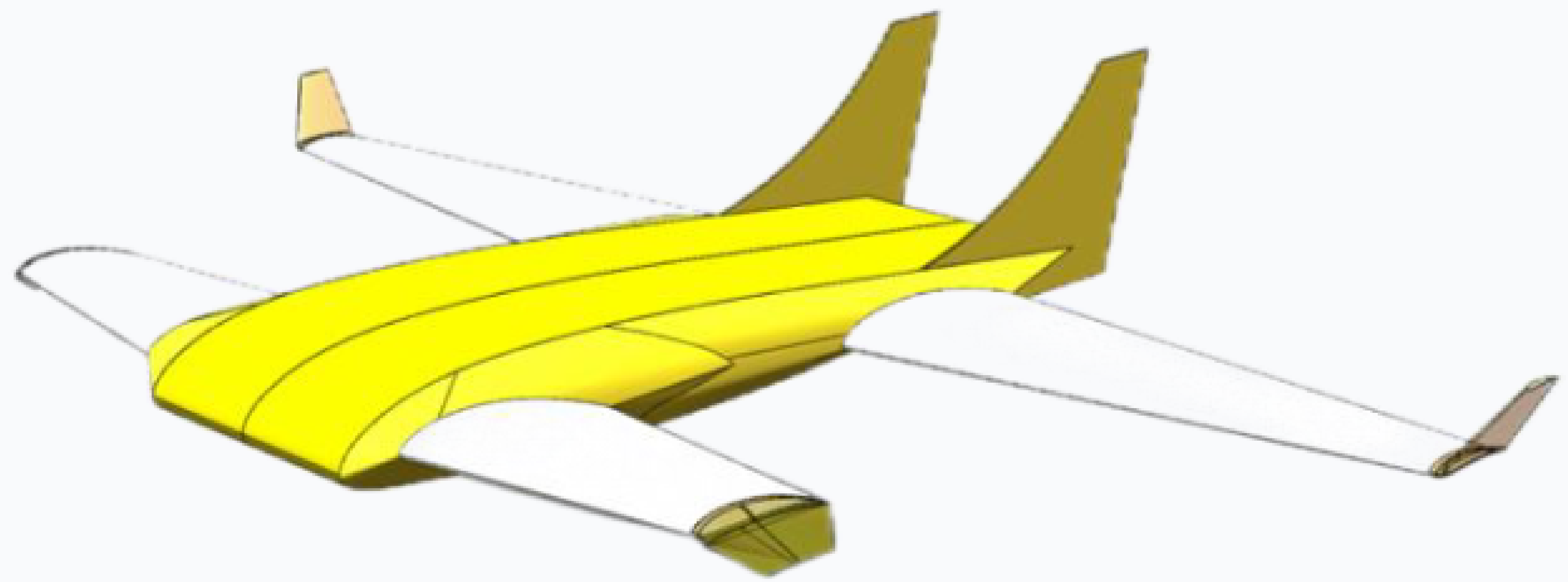

The wide lifting fuselage packaged the payload inside the aerodynamic body. Front and rear wings supplied distributed lift without increasing span beyond the competition envelope.

2. AIRFOIL SCREENING

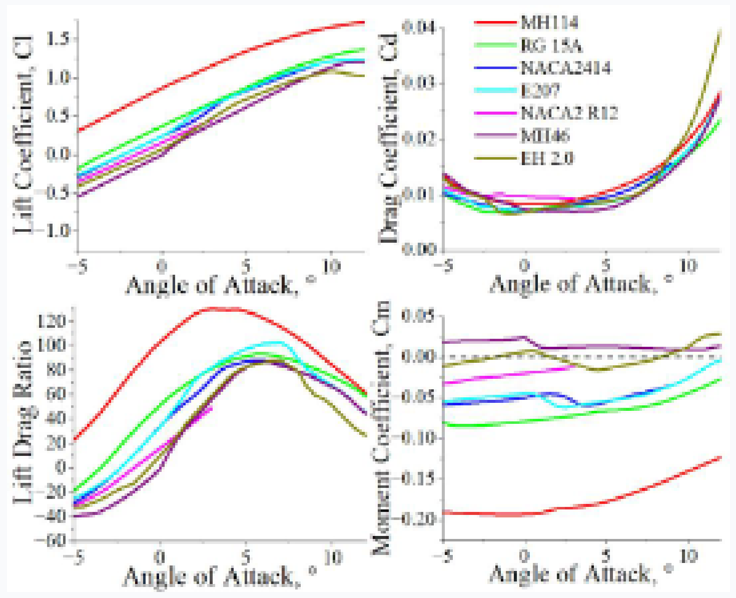

MH114 was selected for low-speed lift. An S-shaped body section reduced the pitching-moment burden of the large lifting fuselage.

3. TANDEM-WING TRIM SETUP

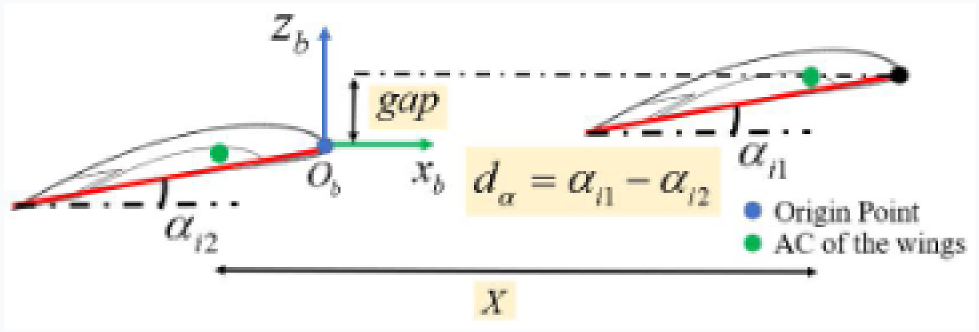

Gap, incidence, and relative wing position became tuning variables for lift distribution and pitch trim.

This step connected packaging constraints to a solvable aerodynamic trim problem.

Tandem-wing lifting-body payload aircraft

Geometry iteration linked wing-body interference, induced drag, and cruise efficiency

4. CFD-DRIVEN DESIGN ITERATION

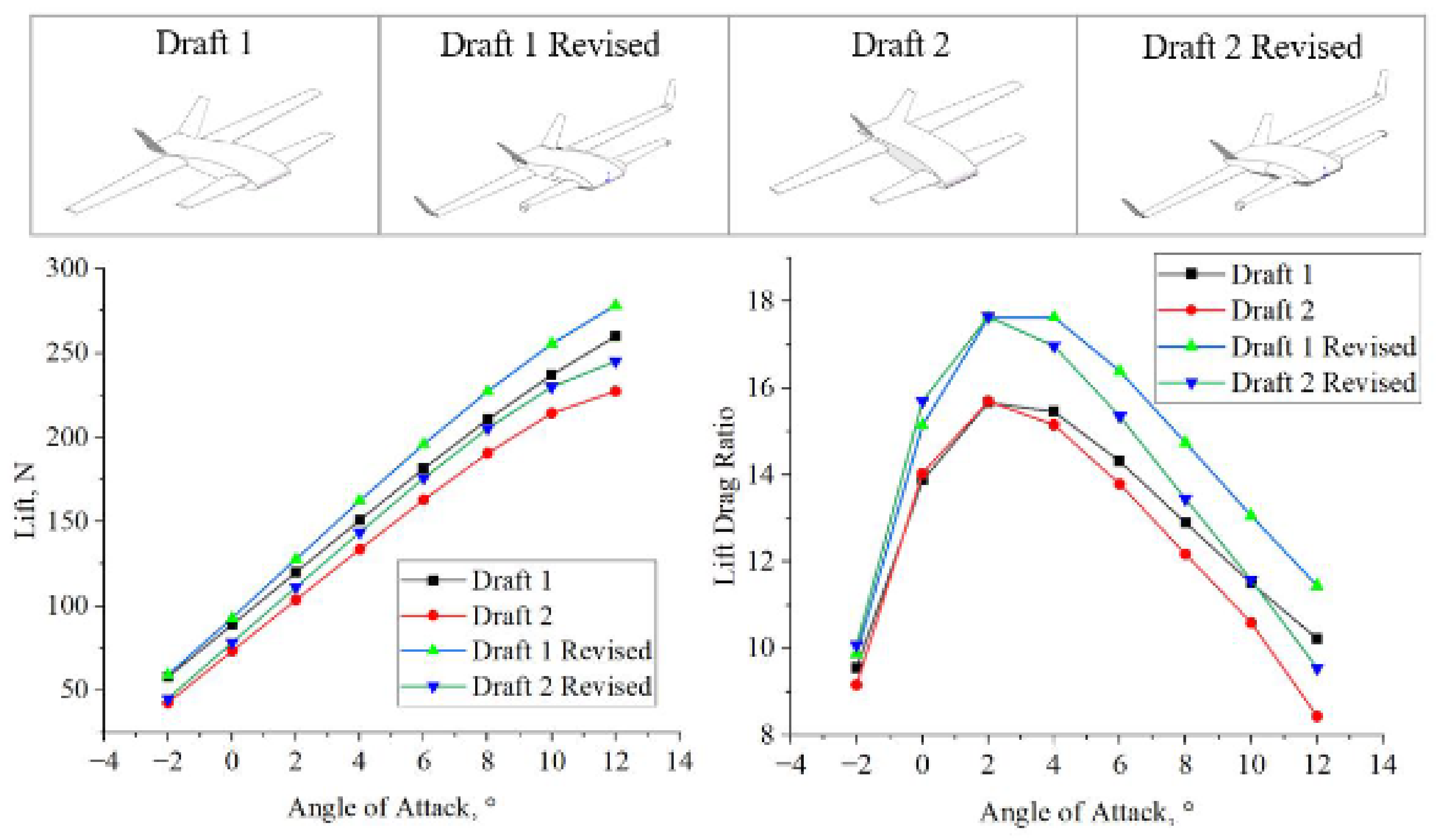

Fluent results compared draft geometries and guided changes to lift, trim, and lift-to-drag performance.

5. REFINEMENT FEATURES

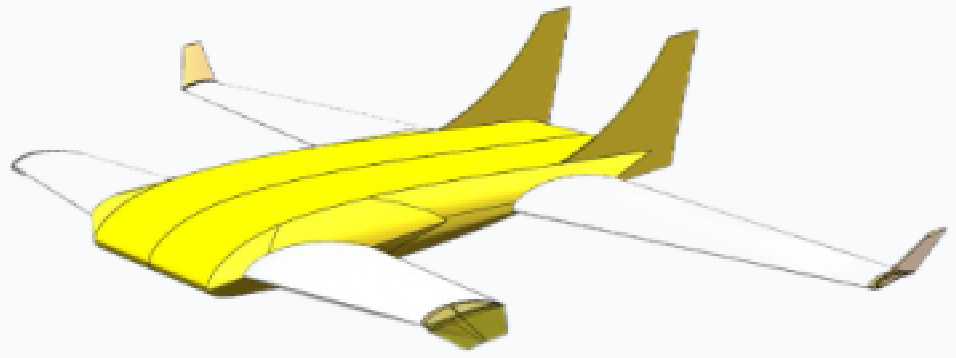

Blended wing-body fairings reduced interference drag around the lifting fuselage.

Front and rear wingtip devices managed tip vortices and induced-drag penalties.

Final cruise performance came from balancing payload volume, trim, and drag.

➢ **The final geometry came from iterative tradeoffs, not from a single styling decision.**

Structural Design

Composite structure matched each component to its load path and manufacturing constraint

COMPOSITE STRUCTURE ARCHITECTURE

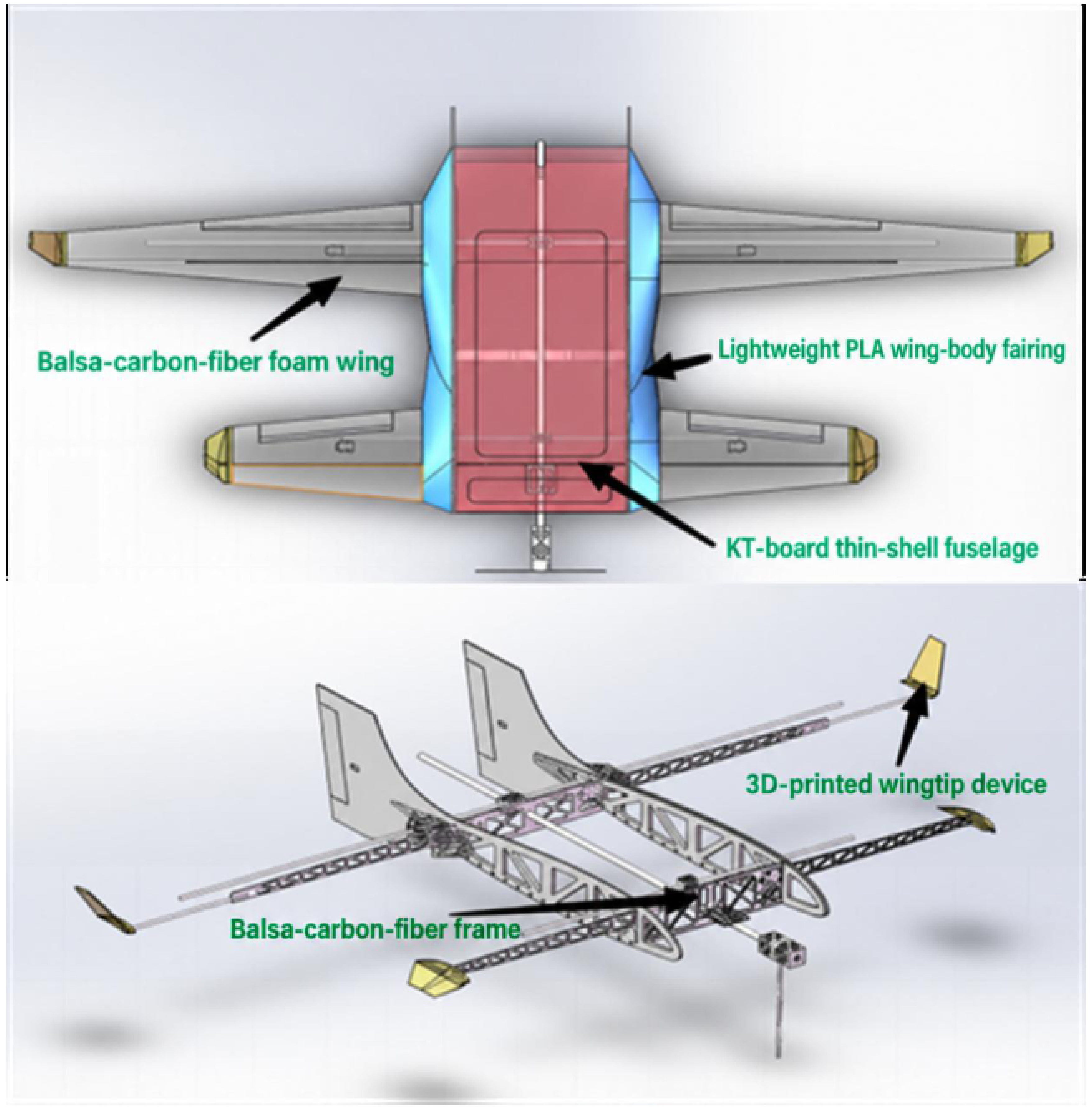

KT-board shell

5 mm thin-shell fuselage for low-cost torsional stiffness and payload volume.

EPP foam wing

Hot-wire foam core preserved airfoil shape and reduced fabrication error.

Balsa-carbon spar

Composite wing spar plus carbon tube resisted lift-induced bending and torsion.

ePLA-LW fairing

3D-printed wing-body fairings formed a closed box around torsion loads.

- Design logic: use inexpensive sheet material for the large fuselage, foam and carbon reinforcement for accurate wings, and printed fairings only where the curved geometry made sheet construction difficult.
- **The result was a low-cost structure with modular fabrication and enough stiffness for heavy-payload flight.**

Manufacturing and Assembly

Thin-shell fuselage, reinforced foam wings, and carbon-tube alignment supported rapid build iteration

FUSELAGE INTERIOR AND LOAD PATH

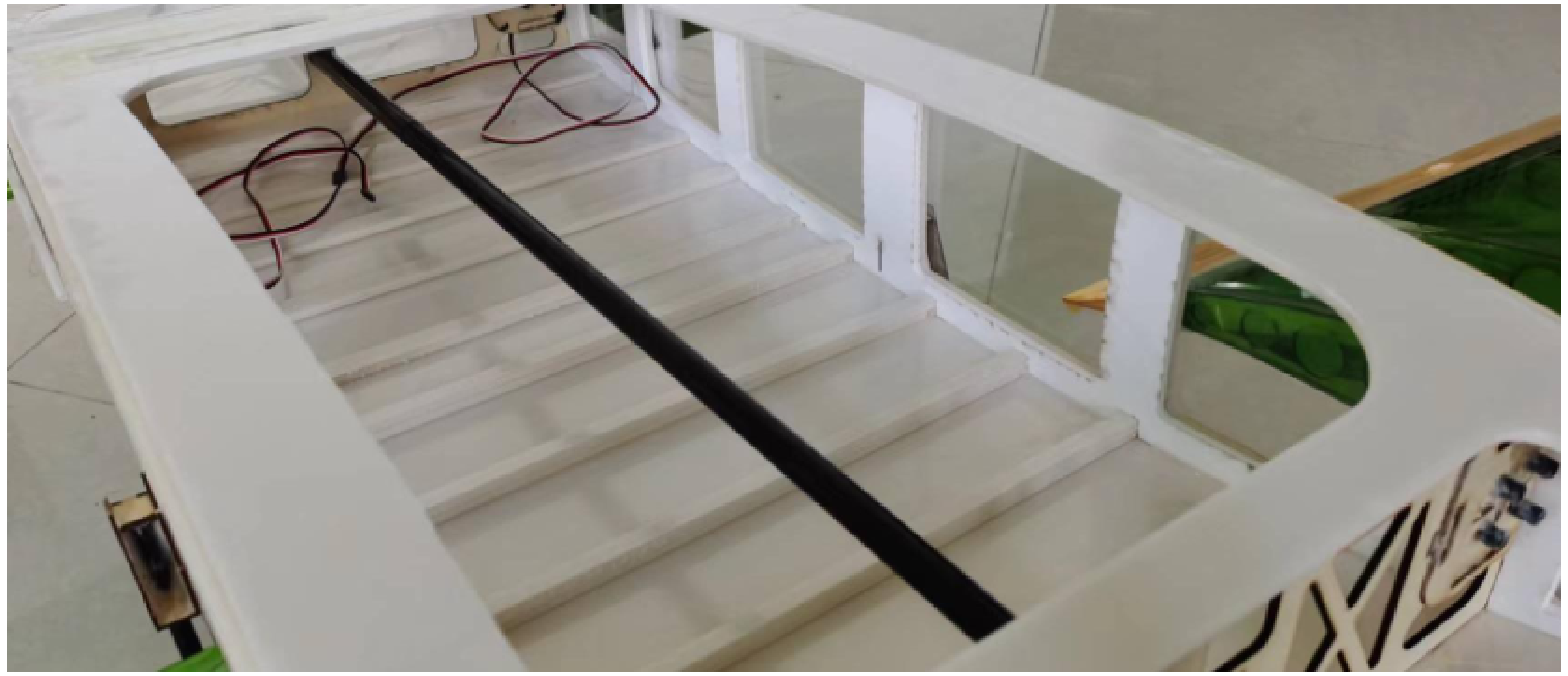

The large lifting body used a KT-board shell with internal ribs and a carbon tube running through the fuselage for alignment and load transfer.

BUILT AIRFRAME

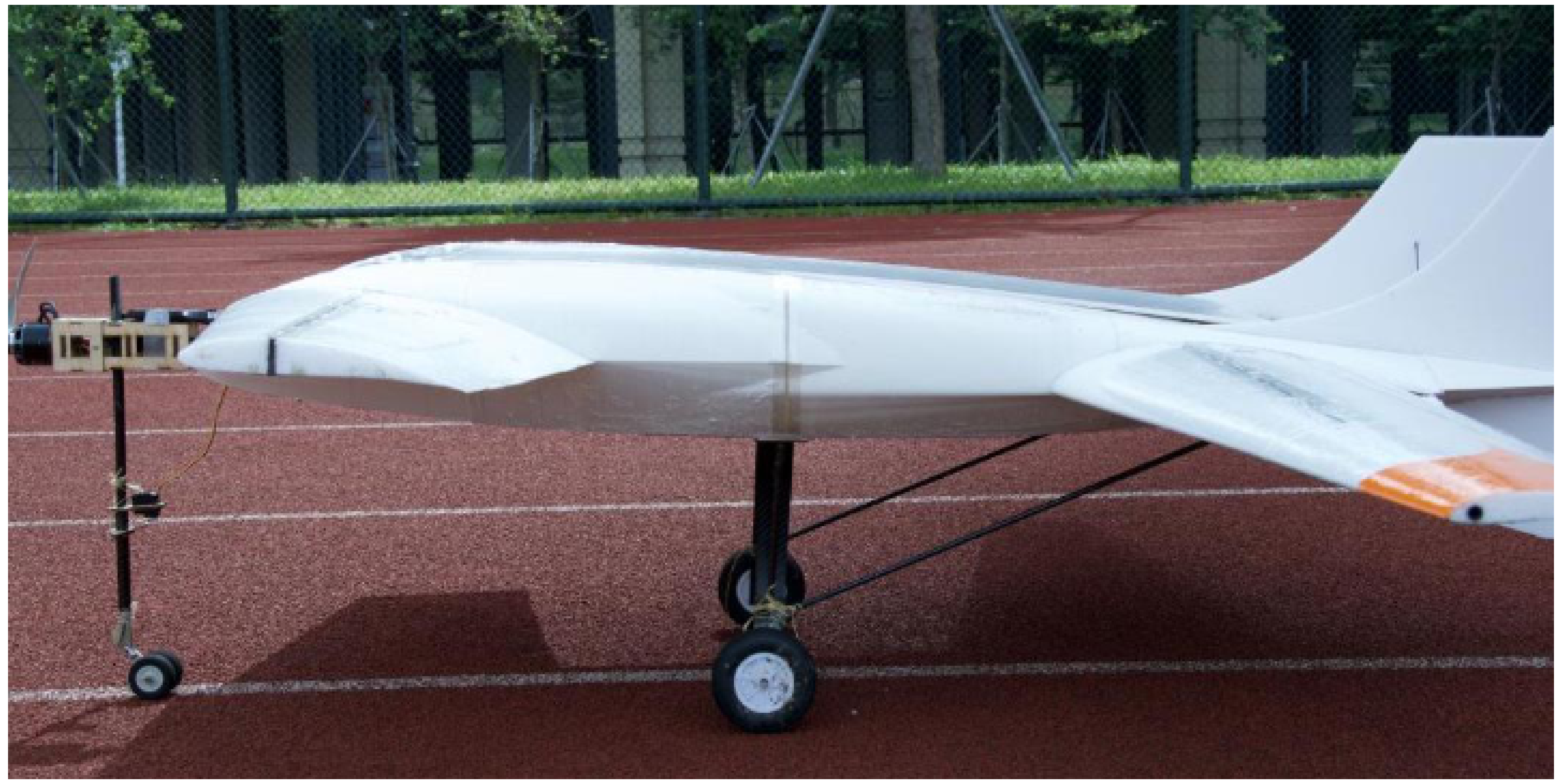

Wing-body fairings connected the front and rear wing roots into a closed structural box around the fuselage.

Thin-shell fuselage

5 mm KT-board skin, side plates, top cover, and ribs improved torsional stiffness.

Reusable wing core

EPP foam wing preserved aerodynamic shape and reduced hand-build variation.

Carbon alignment

17 mm fuselage carbon tube and wing tubes supported repeatable assembly.

Modular joints

Bolted spars and printed connectors made wing installation faster and more accurate.

Flight validation and awards

Video placeholder and award evidence for the tandem-wing lifting-body aircraft

FLIGHT VIDEO

Video slot for takeoff and stable flight footage.

COMPETITION EVIDENCE

National First Prize
Limited-payload flight

National Second Prize
Design report

Additional flight-event award

National Third Prize
Limited-payload flight

Fluid-driven Moving-mass Control Aircraft

Internal fluid transfer shifts the center of mass for coupled roll and pitch control

TWO-DOF CONTROL CONCEPT

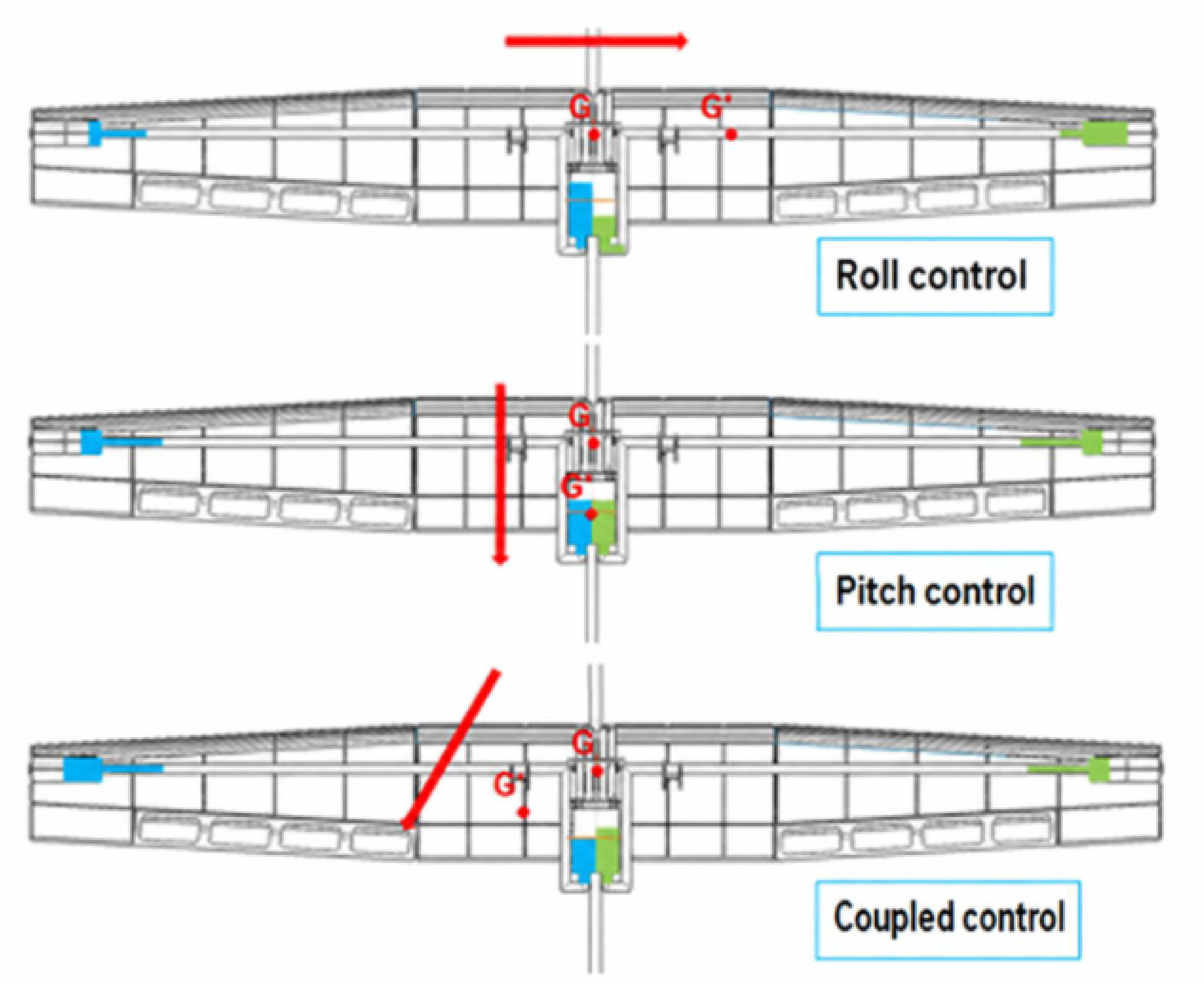

Fluid moves between reservoirs to shift the center of mass. The same mechanism can command roll, pitch, or a coupled roll-pitch response.

WHY MOVING MASS

Conventional control surfaces can add drag, hinge gaps, stealth penalties, and weak control authority at low dynamic pressure. Moving-mass control keeps the external aerodynamic surface cleaner.

CONTROL STATE MAPPING

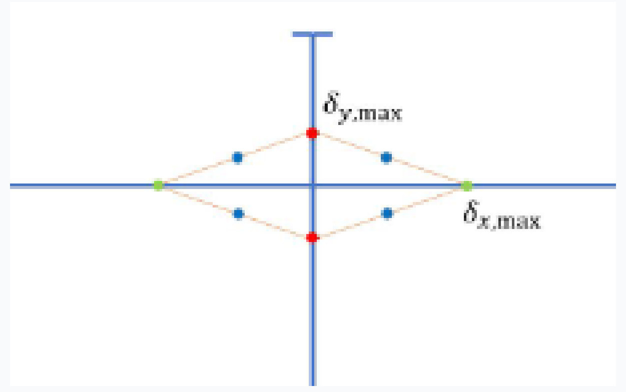

The project mapped discrete fluid-transfer states into an effective input envelope for coupled two-axis control.

Fluid-driven Moving-mass Control Aircraft

Mechanism Design and Prototype Integration

MOVING-MASS MECHANISM（Central）

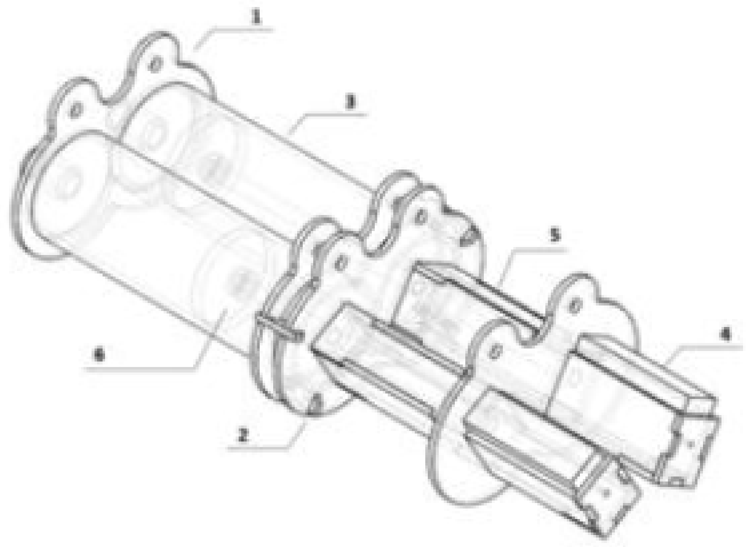

1 - Module connector plate　2 - Structural connector　3 - Central reservoir

4 - Drive unit　5 - Fixed drive mount　6 - Piston linkage

MOVING-MASS MECHANISM（External）

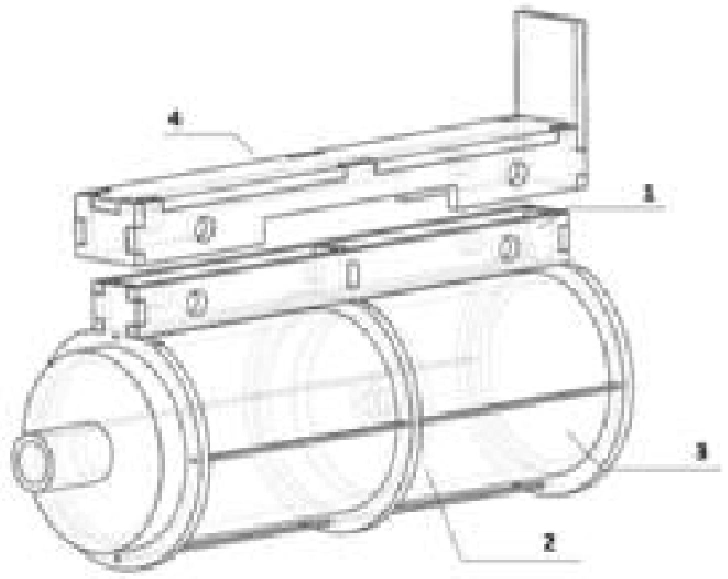

1 - Connector plate (external reservoir)　2 - Piston syringe

3 - External reservoir　4 - Connector plate (wingtip mount)

CAD assembly packaged central reservoirs, drive devices, fixed mounts, and piston-linkage parts into a modular moving-mass unit.

SCALED PROTOTYPE INTEGRATION

(a) Lateral water-driven moving-mass demonstrator installation

(b) External mechanism

(c) Central mechanism

- The prototype mounted external reservoir modules under the wing and a central mechanism inside the fuselage for roll and pitch experiments.
- moving-mass control became a manufacturable mechanism and aircraft prototype.

Indoor wheelchair robot

ROS-based SLAM workflow for indoor mapping and localization

Mapping with Gmapping

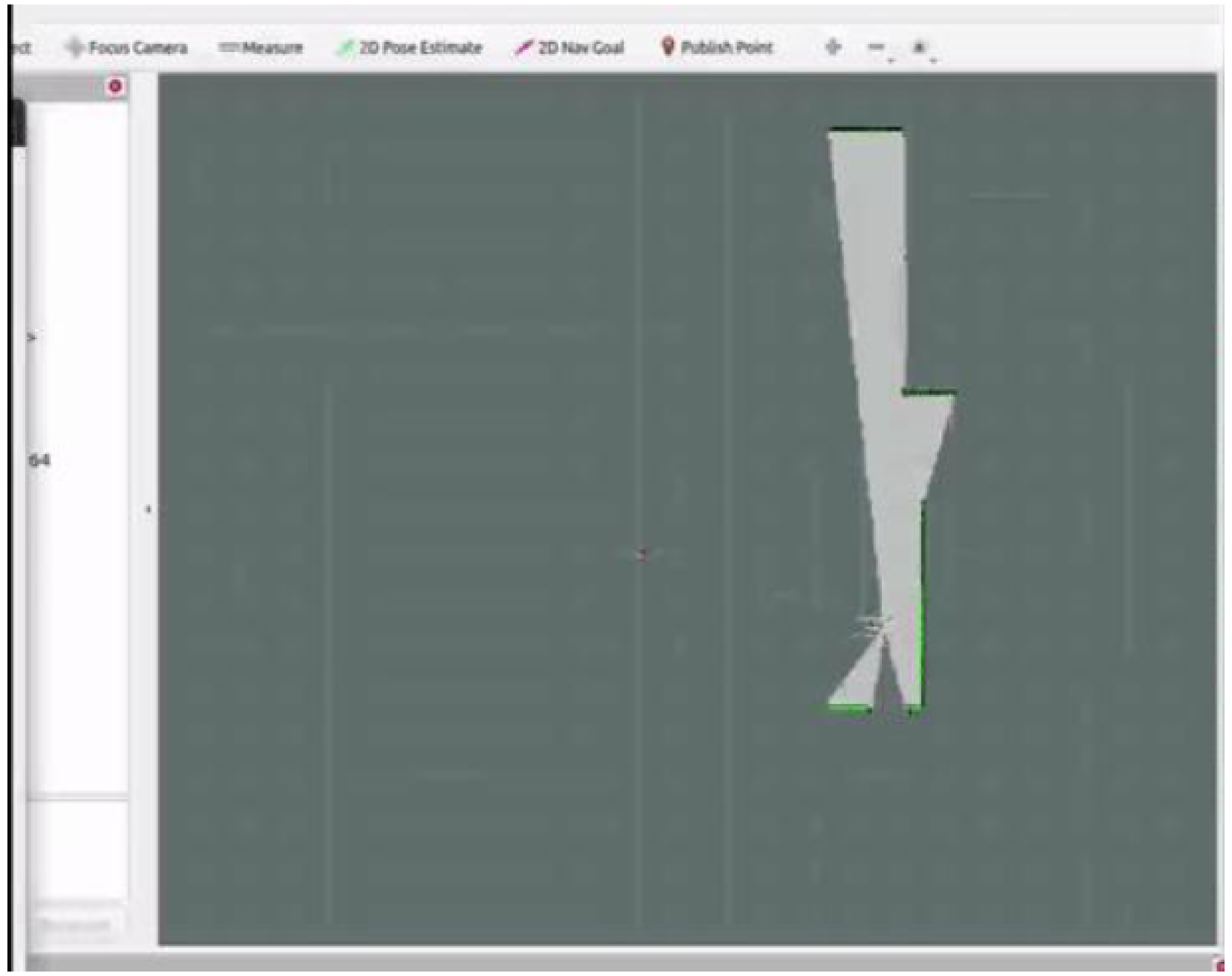

➢ Map construction

Using Gmapping package, LiDAR scans were converted into a 2D occupancy grid so the wheelchair robot could understand the indoor layout.

Localization with AMCL

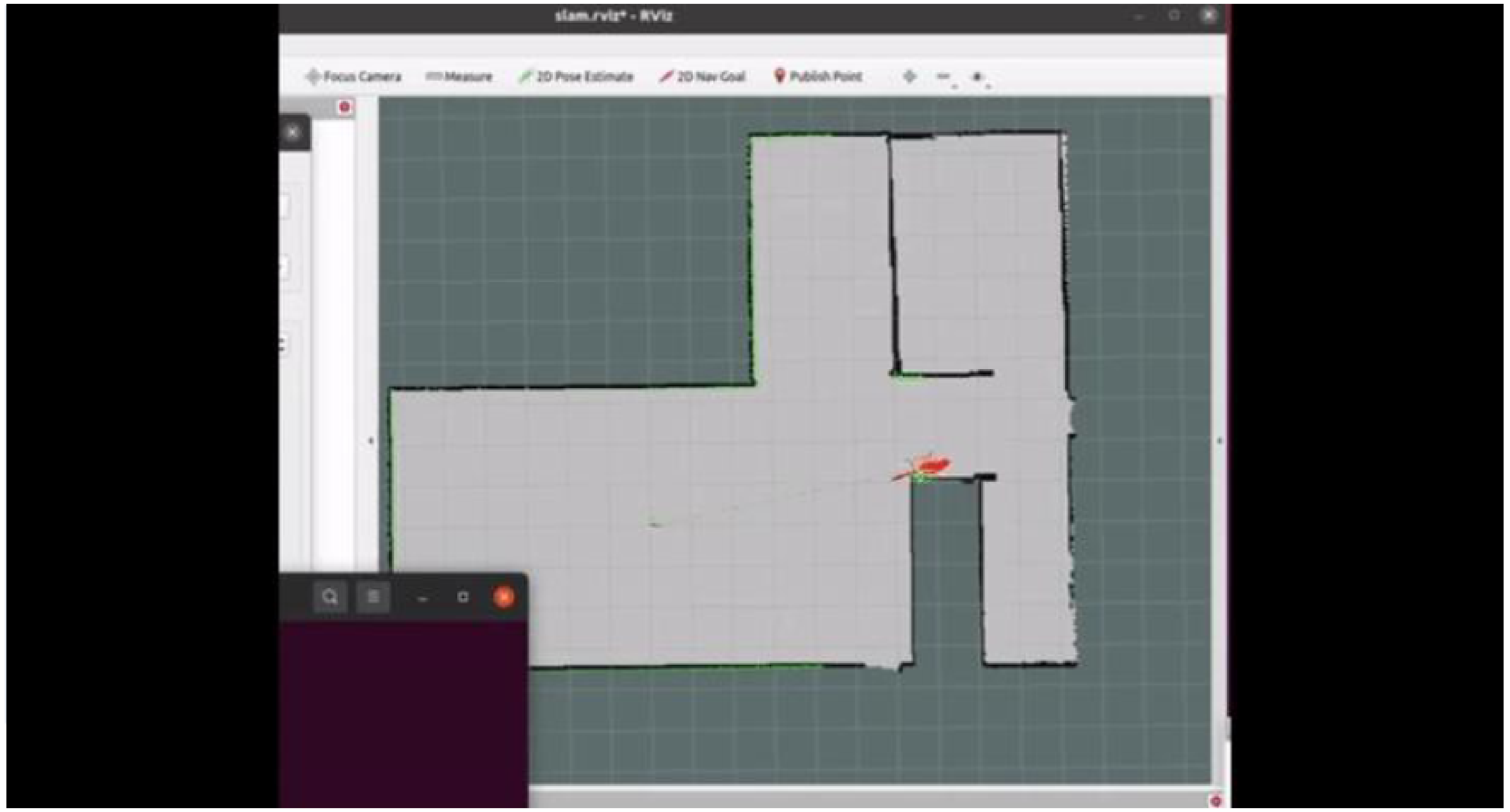

➢ Pose estimation

The adaptive filtering algorithm (using AMCL package) combines the map data and the initial posture of the robot through continuous movement, so that the robot can know its position.

Functions simulation demonstration in Gazebo

Motion studies for navigation and obstacle avoidance

Indoor path planning and navigation

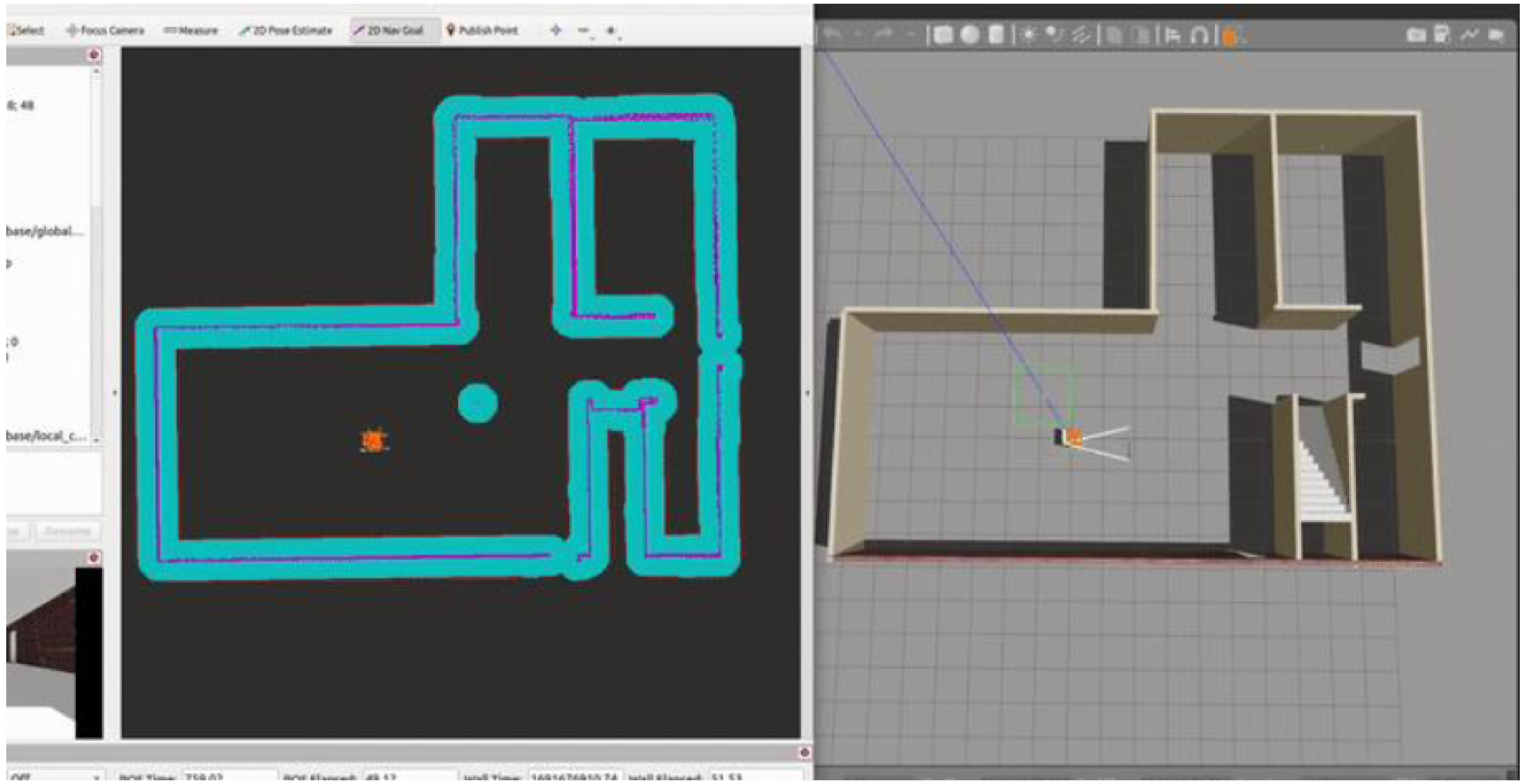

Dynamic obstacle avoidance

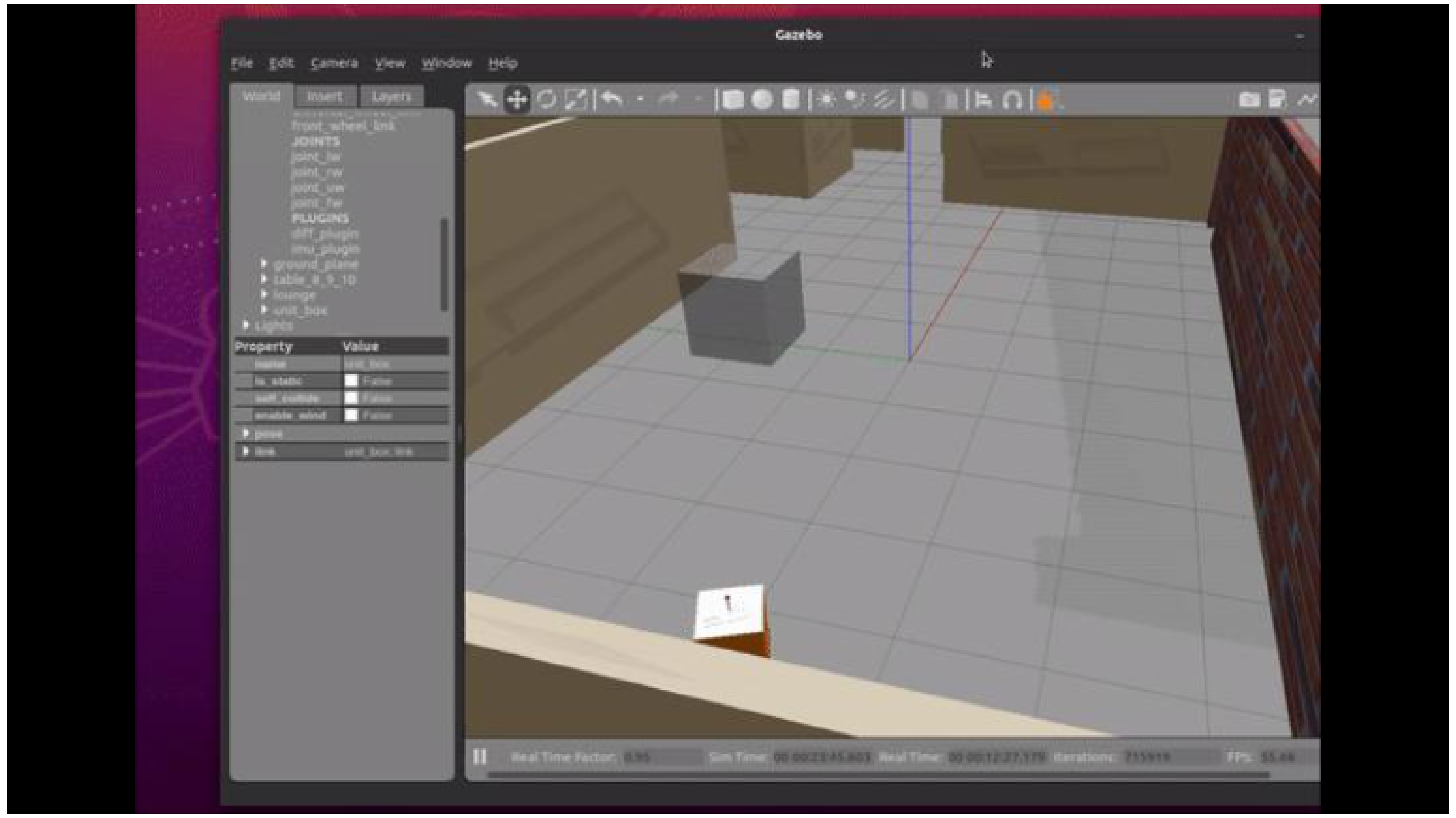

Gazebo connected the robot model, indoor environment, and planner outputs before physical integration.